

# Frictional–collisional equations of motion for granular materials and their application to flow in aerated chutes

By P. NOTT AND R. JACKSON

Department of Chemical Engineering, Princeton University, Princeton, NJ 08544, USA

(Received 12 June 1991 and in revised form 10 February 1992)

Equations of motion and boundary conditions for a flowing granular material, developed in earlier publications, are here extended to allow for drag forces resulting from relative motion of the material and interstitial air. These are solved for fully developed flow down an inclined plane, through which a constant flow of air passes upward. The results are compared with measurements from an experimental aerated chute, in which the inclination of the chute, the flow rate of the granular material, and the flow of air are all varied. Using parameter values from independent measurements, as far as possible, the theory is found to give a good qualitative account of the observed behaviour. With a reasonable assigned value for the one parameter that cannot be determined independently the quantitative agreement is also satisfactory.

---

## 1. Introduction

Two previous papers, Johnson & Jackson (1987) and Johnson, Nott & Jackson (1990), have explored a suggestion of Savage (1982) for a simple method of incorporating frictional effects into a kinetic theory model of the mechanical behaviour of granular materials. The idea is simply to add to the stress given by kinetic theory a separate contribution determined from one or other of the rheological models in the literature of soil mechanics, since these are expected to represent the behaviour at high bulk densities, where there are multiple, long-term contacts between a particle and its neighbours. Clearly this is a very naive way of attempting to treat the behaviour of a granular material over the whole range of bulk densities, but it should give a stress which behaves in the right way at high and low values of the bulk density, and it may catch important aspects of the behaviour at intermediate densities, at least qualitatively.

Johnson & Jackson (1987) applied this model to the plane shearing of a horizontal layer of granular material between plates, compared their predictions with existing experimental results, and were able to show how a layer of non-shearing material occupies the lower part of the space between the plates in most circumstances. Johnson *et al.* (1990) solved the model equations for fully developed flow under gravity down an inclined plane, and compared their predictions with an extensive set of experiments on inclined chutes with base plates of different degrees of roughness.

The present paper reports a further extension of this investigation to the case of a chute equipped with a porous base plate, through which air can be injected. This relieves the gravitational stress that builds up within the layer, and therefore makes fully developed flow possible at lower inclinations than could otherwise be achieved.

A comparison of predictions with experiments on aerated chutes therefore extends the range of conditions over which the consequences of the theory can be tested. In particular, it allows us to study in greater detail the interplay between frictional and collisional components of the stress. In addition, aerated chutes are of technical importance, as they are used to transport particulate materials over moderate horizontal distances. For this purpose a minor extension of the model equations is needed to take account of the drag force exerted on the particles by the air flowing through the interstices. This is described in the next section, after which results of the experiments are presented and compared with the predicted behaviour.

## 2. Mechanical equations for the aerated granular material

The rheological description of the granular material in motion is the same as that used earlier by Johnson *et al.* (1990). The only additional mechanical feature of the present case is the existence of a gas filling the interstices between the particles, and the effect of this will be assumed to be limited to a drag force exerted between the two phases, dependent on their local relative velocity. Modifications of the collisions between particles due to the presence of the gas will be neglected, as will any generation of pseudothermal energy due to the relative motion of gas and particles. Then the equations of motion are as follows. Each phase satisfies a continuity equation

$$\frac{\partial \nu}{\partial t} + \nabla \cdot (\nu \mathbf{u}) = 0, \quad \frac{\partial (1-\nu)}{\partial t} + \nabla \cdot [(1-\nu) \mathbf{u}_g] = 0, \quad (1)$$

where the first refers to the particle phase and the second to the gas,  $\nu$  denotes the volume fraction occupied by particles, and  $\mathbf{u}$  and  $\mathbf{u}_g$  are the velocities of particles and gas, respectively. The momentum equation for the particle phase is

$$\rho_p \nu \frac{D\mathbf{u}}{Dt} = \rho_p \nu \mathbf{g} + \mathbf{f}_{gs} - \nabla \cdot \boldsymbol{\sigma}, \quad (2)$$

where  $\rho_p$  is the intrinsic density of the particulate material,  $\mathbf{g}$  is the specific gravity force vector,  $\mathbf{f}_{gs}$  is the interaction force, per unit total volume, exerted on the particles by the gas, and  $\boldsymbol{\sigma}$  is the particle phase stress tensor. The material derivative is, of course, taken following the particle motion.

Since the density of the gas is much smaller than that of the solid material we omit inertial and gravitational terms from the gas momentum balance, and also neglect shear stresses in the gas phase, other than those associated with the small-scale motion around the particles, which contribute to the drag force. Thus, the gas momentum balance reduces to

$$0 = -\mathbf{f}_{gs} - \nabla p, \quad (3)$$

where  $p$  is the gas pressure. In these equations all variables represent local averages over regions large compared with the particle size.

The particle-phase stress tensor depends quite strongly on the particle temperature, defined by  $T = \frac{1}{3}v^2$ , where  $v^2$  denotes the mean-square fluctuation of the particle velocity about its local average value.  $T$  must then be determined by solution of an equation of balance for the kinetic energy of this pseudothermal motion:

$$\frac{3}{2}\rho_p \nu \frac{DT}{Dt} = -\nabla \cdot \mathbf{q}_{pt} - \boldsymbol{\sigma}_c : \nabla \mathbf{u} - I. \quad (4)$$

Here  $\mathbf{q}_{\text{pt}}$  denotes the flux of pseudothermal energy,  $I$  denotes its rate of dissipation, per unit total volume, in inelastic collisions, and  $\boldsymbol{\sigma}_{\text{c}}$  is the collisional part of the particle phase stress (see below).

As in the work of Johnson *et al.* (1990) we attempt to account for contributions to the particle-phase stress from both brief collisions between pairs of particles, and longer term sliding and rolling contacts, by the crude device of combining these contributions additively, with each calculated as though it acted alone. This proved quite successful in representing the behaviour of a chute without aeration. Thus, we write

$$\boldsymbol{\sigma} = \boldsymbol{\sigma}_{\text{c}} + \boldsymbol{\sigma}_{\text{r}}. \quad (5)$$

For the collisional contribution  $\boldsymbol{\sigma}_{\text{c}}$ , the pseudo-thermal energy flux  $\mathbf{q}_{\text{pt}}$ , and the dissipation function  $I$  we use expressions derived by Lun *et al.* (1984) from dense-gas kinetic theory, which are correct when the coefficient of restitution for collisions between pairs of particles is close to unity. These are simplified, as suggested by Jenkins (1987), by replacing the coefficient of restitution  $e$  by unity everywhere except in the dissipation function  $I$ , which is itself of order  $1 - e$ . Jenkins argues that this should be done to maintain consistency in orders of approximation, and in practice it scarcely changes the results of the computations. Thus

$$\begin{aligned} \boldsymbol{\sigma}_{\text{c}} = & [\rho_{\text{p}} \nu T (1 + 4\nu g_0) - \mu_{\text{b}} \nabla \cdot \mathbf{u}] \mathbf{I} \\ & - \frac{1}{3}(2 + \alpha) \left[ \frac{2\mu}{g_0} (1 + \frac{8}{5}\nu g_0)^2 + \frac{6}{5}\mu_{\text{b}} \right] \mathbf{S}, \end{aligned} \quad (6)$$

$$\mathbf{q}_{\text{pt}} = -\frac{\lambda}{g_0} \left[ \left(1 + \frac{12}{5}\nu g_0\right)^2 + \frac{512}{25\pi} (\nu g_0)^2 \right] \nabla T \quad (7)$$

and 
$$I = \frac{12}{\pi^{\frac{1}{2}}} (1 - e^2) \frac{\rho_{\text{p}} \nu^2}{d} g_0 T^{\frac{3}{2}}, \quad (8)$$

where 
$$\mu = \frac{5m(T/\pi)^{\frac{1}{2}}}{16d^2}, \quad \mu_{\text{b}} = \frac{256\mu\nu^2 g_0}{5\pi}, \quad \lambda = \frac{75m(T/\pi)^{\frac{1}{2}}}{64d^2}. \quad (9)$$

$\mathbf{S}$  denotes the rate of deformation tensor for the velocity field  $\mathbf{u}$ , and  $m$  and  $d$  are the mass and diameter of individual particles, respectively. The radial distribution function  $g_0$  is chosen as

$$g_0 = \frac{1}{(1 - (\nu/\nu_0)^{\frac{1}{3}})}, \quad (10)$$

where  $\nu_0$  is the volume fraction of solids at random close packing, taken to be 0.65 in this work. This form constrains the solids fraction to remain smaller than  $\nu_0$ . The dimensionless constant  $\alpha$  in (6) is assigned the value 2. These choices for  $g_0$  and  $\alpha$  ensure consistency with earlier work on chute flow (Johnson *et al.* 1990). The form (10) for  $g_0$  ensures that the stress will diverge as the volume fraction approaches close packing, thus preventing  $\nu$  from assuming an unphysically large value. For consistency with the kinetic theory of dilute gases it can be shown that  $\alpha$  should tend to unity when  $e_{\text{p}} \rightarrow 1$  and  $\nu \rightarrow 0$ , but this would give rather low values for the stress at more realistic volume fractions.

The literature of soil mechanics contains many proposed expressions for  $\boldsymbol{\sigma}_{\text{r}}$ , the ‘frictional’ contribution to the stress but fortunately, for the case of plane shear

considered here, they all reduce to the Coulomb relation  $T_f = N_f \sin \phi$ , where  $T_f$  and  $N_f$  are the shear stress and the normal stress, respectively, on the planes of shear, and  $\phi$  is a property of the granular material called its angle of internal friction. The volume fraction  $\nu$  and the normal stress  $N_f$  are related, with the stress increasing rapidly and diverging as  $\nu \rightarrow \nu_0$ . Following Johnson *et al.* (1990) we take

$$\begin{aligned} N_f &= Fr \frac{(\nu - \nu_1)^P}{(\nu_0 - \nu)^N} \quad \text{for } \nu > \nu_1 \\ &= 0 \quad \text{for } \nu \leq \nu_1, \end{aligned} \quad (11)$$

where  $Fr$ ,  $P$  and  $N$  are constants characteristic of the material. This gives a vanishing frictional contribution to the stress for sufficiently small values of  $\nu$ .

To complete the closure of the equations of motion an expression is needed for the drag force  $\mathbf{f}_{gs}$ , and this is taken as a weighted combination of the well-known Ergun and Richardson–Zaki equations, the former of which is well established for flow of gas through a packed bed of high solid volume fraction, while the latter has the right behaviour at small values of the volume fraction. Thus

$$\mathbf{f}_{gs} = w \left[ \frac{150\mu_g (\mathbf{u}_g - \mathbf{u}) \nu^2}{d^2 (1-\nu)^3} + \frac{1.75\rho_g |\mathbf{u}_g - \mathbf{u}| (\mathbf{u}_g - \mathbf{u}) \nu}{d(1-\nu)^3} \right] + (1-w) \left[ \frac{\rho_s g (\mathbf{u}_g - \mathbf{u}) \nu}{u_t (1-\nu)^{n-1}} \right]. \quad (12)$$

The Richardson–Zaki exponent  $n$  depends on the Reynolds number of a particle at the velocity  $u_t$  of free fall in the gas. In this work  $u_t = 7.5$  m/s and  $n = 3.4$ , corresponding to the 1 mm glass beads used in the experiments. The weighting factor  $w$  is a function of  $\nu$  chosen so that  $w \rightarrow 0$  when  $\nu \rightarrow 0$ , while  $w$  approaches unity as  $\nu \rightarrow \nu_0$ ; specifically we took

$$w = \exp\left(-10 \frac{\nu_0 - \nu}{\nu}\right), \quad (13)$$

with which the transition from the Ergun to the Richardson–Zaki form occurs rather sharply around  $\nu = 0.5$ .

The above equations are subject to boundary conditions at solid surfaces (in this case the base of the chute) and at free boundaries beyond which the particle concentration vanishes. At the solid boundary the conditions on the particle velocity and the particle temperature formulated by Johnson *et al.* (1990) can be taken over unchanged:

$$\mathbf{n} \cdot \boldsymbol{\sigma} \cdot \frac{\mathbf{u}_{sl}}{|\mathbf{u}_{sl}|} + N_f(\nu) \tan \delta + \frac{\phi' \sqrt{3\pi\rho_p \nu T^{\frac{1}{2}} |\mathbf{u}_{sl}|}}{6\nu_0 [1 - (\nu/\nu_0)^{\frac{1}{3}}]} = 0 \quad (14)$$

and

$$\mathbf{n} \cdot \mathbf{q}_{pt} = \frac{\sqrt{3\pi\nu\rho_p} T^{\frac{1}{2}}}{2\nu_0 [1 - (\nu/\nu_0)^{\frac{1}{3}}]} \left\{ \frac{\phi' |\mathbf{u}_{sl}|^2}{3} - \frac{T(1 - e_w^2)}{2} \right\}. \quad (15)$$

Here  $\mathbf{n}$  denotes the unit normal to the solid boundary, drawn into the particulate material,  $\mathbf{u}_{sl}$  is the slip velocity at the wall, defined as  $\mathbf{u} - \mathbf{u}_w$ , where  $\mathbf{u}_w$  is the velocity of the wall,  $e_w$  is the coefficient of restitution for collisions between particles and the wall, and  $\delta$  is the angle of friction for particulate material sliding over the wall. The factor  $\phi'$ , which we call the specularity coefficient, is a measure of the average fraction of tangential momentum of a particle lost in a collision with the wall. It approaches zero when the wall is perfectly smooth and the rebound of particles is specular, but approaches unity for perfectly diffuse rebounds at a rough wall. In (14)

the second and third terms represent the frictional force opposing sliding over the wall, and the rate of transfer of tangential momentum to the wall during collisions, respectively. In (15) the first term on the right-hand side represents the rate of working of collisional stresses at the wall, while the second represents the rate of dissipation of pseudo-thermal energy in inelastic collisions between particles and the wall.

At a free surface of the particulate material the normal flux of pseudothermal energy must vanish, of course:

$$\mathbf{n} \cdot \mathbf{q}_{pt} = 0 \quad (16)$$

and the particle phase stress  $\boldsymbol{\sigma}$  should also be required to vanish. However, this requires that  $\nu \rightarrow 0$  at the surface and, when the bulk of the particle assembly has high density, this leads to a very steep gradient of  $\nu$  immediately adjacent to the surface, and consequent problems of stiffness in solving the equations of motion numerically. As a practical matter, therefore, we avoid this by writing a force balance for the uppermost layer of particles separately, then apply our continuum equations to the rest of the material below this layer. For the continuum equations, therefore, the stress at the upper boundary of the domain of integration is the (non-zero) stress below the topmost layer of particles. Johnson *et al.* (1990) showed that the relation between this and the weight of the particles in the topmost layer is

$$\mathbf{n} \cdot \boldsymbol{\sigma} = \frac{1}{8} \pi \rho_p d (\nu / \nu_0)^{\frac{3}{2}} \mathbf{g} \quad (17)$$

which follows from an assumption that the average area per particle in this layer is approximately  $d^2$  at random close packing. This method of handling the free-surface boundary condition can be justified *a posteriori* by comparing computed results with predictions of more elaborate computations which do not even assume the existence of a sharply defined upper surface (Johnson *et al.* 1990).

For the particular case of fully developed flow under gravity down an aerated chute, inclined at an angle  $\theta$  to the horizontal, the equations can be reduced to explicit dimensionless forms as follows. The component of the momentum balance normal to the base of the chute is

$$\frac{d}{dY} [N_r^* + f_1 T^*] = \left(\frac{H}{d}\right) [-\nu + f_{gs}^*], \quad (18)$$

the component of momentum balance parallel to the base is

$$\frac{d}{dY} \left[ \frac{N_r^* \sin \phi}{\tan \theta} + \frac{f_2 T^{*\frac{1}{2}}}{((H \tan \theta)/d)^{\frac{1}{2}}} \frac{du^*}{dY} \right] = -\left(\frac{H}{d}\right) \nu, \quad (19)$$

and the balance of pseudothermal energy is

$$\frac{d}{dY} \left[ f_3 T^{*\frac{1}{2}} \frac{dT^*}{dY} \right] + \frac{H}{d} \tan \theta f_2 T^{*\frac{1}{2}} \left( \frac{du^*}{dY} \right)^2 - \left(\frac{H}{d}\right) f_5 T^{*\frac{3}{2}} = 0. \quad (20)$$

In the above equations  $H$  is the depth of the flowing layer of particulate material and the coordinate  $y$  is measured normal to the base of the chute from an origin in the base. A dimensionless coordinate  $Y$  is defined as  $y/H$ , and other dimensionless variables, distinguished by stars, are defined as follows:

$$u^* = \frac{u}{(gH \sin \theta)^{\frac{1}{2}}}; \quad T^* = \frac{T}{gd \sin \theta}; \quad N_r^* = \frac{N_r}{\rho_p gd \cos \theta}; \quad f_{gs}^* = \frac{f_{gs}}{\rho_p g \cos \theta}.$$

The dimensionless drag force is then given by

$$f_{gs}^* = w \left[ 150 \mu_g^* v^* \frac{\nu^2}{(1-\nu)^3} + 1.75 \rho_g^* (v^* u_{mf}^*)^2 \frac{\nu}{(1-\nu)^3} \right] + (1-w) \frac{v^*}{v_t^* \cos \theta} \frac{\nu}{(1-\nu)^{n-1}}, \quad (21)$$

where  $v_t^* = u_t/u_{mf}$  and

$$\mu_g^* = \frac{\mu_g u_{mf}}{\rho_p g d^2 \cos \theta}; \quad v^* = \frac{u_g}{u_{mf}}; \quad \rho_g^* = \frac{\rho_g}{\rho_p}; \quad u_{mf}^* = \frac{u_{mf}}{(g d \cos \theta)^{1/2}}; \quad f_{gs}^* = \frac{f_{gs}}{\rho_p g \cos \theta}.$$

The boundary condition (14) at the chute base takes the form

$$\frac{f_2 T^{*1/2}}{(H \tan \theta / d)^{1/2}} \frac{du^*}{dY} + \frac{N_f^* [\sin \phi - \tan \delta]}{\tan \theta} = \frac{\pi}{2\sqrt{3}} \left( \frac{H}{d \tan \theta} \right)^{1/2} \frac{\nu g_0}{\nu_0} \phi' u^* T^{*1/2} \quad (\text{at } Y = 0), \quad (22)$$

while the condition (15) becomes

$$\frac{4\nu_0 f_3}{\pi \sqrt{3\nu g_0}} \frac{dT^*}{dY} = \frac{H}{d} (1 - e_w^2) T^* - \frac{2}{3} \left( \frac{H}{d} \right)^2 \phi' \tan \theta u^{*2} \quad (\text{at } Y = 0). \quad (23)$$

The normal and tangential components of the stress boundary condition (17) at the free surface can be written

$$f_1 T^* + N_f^* = \frac{1}{6} \pi (\nu / \nu_0)^{3/2} \quad (\text{at } Y = 1) \quad (24)$$

and

$$\frac{f_2 T^{*1/2}}{((H \tan \theta) / d)^{1/2}} \frac{du^*}{dY} + \frac{N_f^* \sin \phi}{\tan \theta} = \frac{1}{6} \pi (\nu / \nu_0)^{3/2} \quad (\text{at } Y = 1), \quad (25)$$

while the thermal flux condition is

$$\frac{dT^*}{dY} = 0 \quad (\text{at } Y = 1). \quad (26)$$

In the above equations  $f_1, f_2, f_3$  and  $f_5$  denote the following dimensionless functions of  $\nu$ :

$$f_1(\nu) = \nu(1 + 4\nu g_0),$$

$$f_2(\nu) = \frac{(2 + \alpha) 5\pi^{1/2}}{288g_0} (1 + \frac{8}{5}\nu g_0)^2 + \frac{8(2 + \alpha)\nu^2 g_0}{15\pi^{1/2}},$$

$$f_3(\nu) = \frac{25\pi^{1/2}}{128g_0} (1 + \frac{12}{5}\nu g_0)^2 + \frac{4}{\pi^{1/2}} \nu^2 g_0,$$

$$f_5(\nu) = \frac{12}{\pi^{1/2}} (1 - e^2) \nu^2 g_0.$$

In formulating the above equations for chute flow only the component of the gas-particle drag force normal to the plane of the chute has been taken into account; in other words, it has effectively been assumed that the component of the velocity of the gas in the direction of motion of the solid material is everywhere equal to the velocity of the particles. This cannot be entirely true, since the air emerges from the base of the chute with a vanishing value for this component of velocity, and the air

above the free surface of the moving layer of particles also exerts some drag at the surface. However, Nott (1991) has shown that these effects would be expected to be negligibly small for the systems studied here.

### 3. Method of solution

Before embarking on numerical solution it is useful to reduce the order of the system by integrating each of (19) and (20) once with respect to  $Y$ . Incorporating the free-surface boundary conditions (24) and (25) we thus obtain

$$N_f^* + f_1 T^* = \left(\frac{H}{d}\right) \int_Y^1 (\nu - f_{gs}^*) dY + \frac{\pi}{6} \left(\frac{\nu(Y=1)}{\nu_0}\right)^{\frac{3}{2}} \quad (27)$$

$$\text{and} \quad N_f^* \sin \phi + f_2 \left[\frac{T^* \tan \theta}{H/d}\right]^{\frac{1}{2}} \frac{du^*}{dY} = \tan \theta \left\{ \left(\frac{H}{d}\right) \int_Y^1 \nu dY + \frac{\pi}{6} \left(\frac{\nu(Y=1)}{\nu_0}\right)^{\frac{3}{2}} \right\}. \quad (28)$$

These two equations then replace (19), (20), (24) and (25). The system of equations (20), (27) and (28), together with the boundary conditions (22), (23) and (26), is then solved by a finite-difference method. The interval  $[0, 1]$  for  $Y$  is divided into  $N$  equal sub-intervals, so that there are  $N-1$  interior points and the two boundary points. The derivatives are then replaced by finite-difference approximations with errors of  $O(\Delta Y^2)$ , using central differences at the interior points and forward or backward differences at the boundary points. The integrals in (27) and (28) are approximated using Simpson's rule to maintain the  $O(\Delta Y^2)$  truncation error. The resulting set of algebraic equations for the values of the dependent variables at the grid points is solved by the Newton-Raphson method. Further details of this procedure are given by Nott (1991). This procedure converged much more rapidly than that used earlier by Johnson *et al.* (1990). In practice  $N = 31$  proved adequate for all the cases studied.

The Newton-Raphson method has quadratic convergence from a sufficiently good starting point, but often fails to converge if the starting approximation is poor. Thus, once a solution has been obtained for one pair of values of the parameters  $\theta$  and  $H/d$ , it is best to continue this by successive small changes in one or other of these parameters. In particular, by generating solutions for a sequence of closely spaced values of  $H/d$ , we can find how the mass flow rate varies with the depth of the flowing layer on a chute of given inclination. This method of continuation fails if a limit point or a bifurcation point is encountered, where the Jacobian needed in the Newton-Raphson procedure vanishes. This can occur in systems of this sort, so the solutions were actually continued using the AUTO software package (Doedel 1986), which uses arclength along the branch of solutions being followed as a continuation parameter, and is capable of following the branch through singular points where the Jacobian vanishes.

### 4. Experimental apparatus and procedure

The granular material used in this work consists of glass beads of 1 mm nominal diameter. These are spherical in shape and the manufacturer's tolerance on the diameter is 10%, so they resemble closely the identical, hard spheres treated by the theory of Lun *et al.* (1984).

The chute is a modified version of that used by Johnson *et al.* (1990), the main difference being the replacement of the base plate by a porous plate backed by a

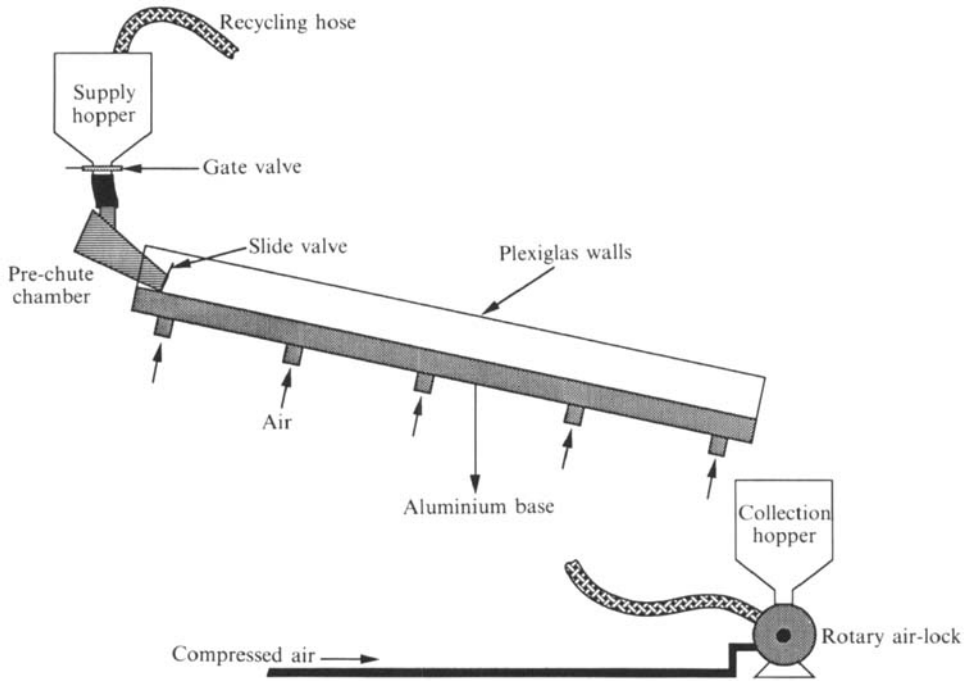


FIGURE 1. Overall arrangement of the experimental apparatus.

windbox, as indicated in figure 1, so that the flowing material can be aerated. The flowing material is recycled to the feed hopper using a rotary air lock and a pneumatic lift line, as shown. The chute is 135 cm long and 6 cm wide, and is bounded laterally by Plexiglas walls. Clean, dry air for aeration is provided by a blower with a maximum volumetric delivery of 2000 ft<sup>3</sup>/min and a shut off head of 18 in. of water.

The most critical aspect of the design of the apparatus is the choice of a suitable porous plate for the chute base. This must be stiff enough to support the weight of the particulate material without flexing appreciably, and it must have absolutely uniform permeability to the passage of gas, so that the air is uniformly distributed over the length and width of the chute. After a number of unsuccessful trials it was found that the properties required could be found in certain porous plastic sheets. For the present purpose a  $\frac{1}{8}$  in. thick sheet of porous polypropylene was found to be most suitable. The average pore size is 125  $\mu\text{m}$  and the material is more rigid than others that were tested, giving a higher coefficient of restitution  $e_w$ . Also the surface is quite smooth, so the angle of wall friction  $\delta$  is not too large.

The depth of the flowing layer is determined with a small, vertical impact plate that can be positioned above the surface of the material with a machinist's dial micrometer. It is lowered until particles can be seen to be hitting its lower edge. Provision is also made for measuring the mass holdup; that is, the mass of material per unit area of the chute base in the fully developed flowing layer. This is found by lowering two plates rapidly and simultaneously into the material so as to stop the flow, then weighing the material trapped between them. The mass flow rate is measured by collecting and weighing the material leaving the end of the chute in a measured time interval.

The behaviour of the chute is found to be quite sensitive to its angle of inclination,

and this is measured by a vernier protractor clamped to the chute and supporting a sensitive bubble level. This arrangement can determine the inclination within  $0.05^\circ$ . The downstream end of the chute is supported by a wire span attached to a ratchet winch, so the inclination can be changed by winching this end up or down.

Provision was made for measuring velocity profiles using a fibre-optic probe, as described by Johnson *et al.* (1990). The measurements were repeatable within 5%, but the velocity profiles measured are those of material in contact with the sidewall of the chute. They are therefore of limited value, and are not reported here. (They can, however, be found in Nott 1991.) The probe can also be used to measure the lateral profile of velocity of particles in the free upper surface, and two such profiles are shown in figure 6.

The material is fed from the storage hopper to the upper end of the chute in two stages. It first falls freely from the hopper exit into a pre-chute chamber, seen in figure 1, and this flow is controlled by a gate valve at the hopper exit. Flow from the pre-chute chamber into the chute proper can then be controlled separately by a slide valve at the exit from the chamber. This arrangement was introduced by Johnson *et al.* as a means of controlling the condition of the granular material entering the chute. If the slide valve is opened wide and the flow of material controlled entirely by the gate valve at the hopper exit, the material enters the chute in an energetic, low-density state after falling freely then bouncing on the base of the pre-chute chamber. On the other hand, if the flow is controlled with the slide valve, using the gate valve only to keep the pre-chute chamber full of granular material, the material enters the chute in a dense, low-energy state. With a smooth chute base Johnson *et al.* found that different, apparently fully developed flow regimes could be generated by using the two different methods of feeding the material. With a rougher base, on the other hand, the lower-density flowing layer obtained by controlling the flow at the hopper exit usually collapsed to a high-density layer before leaving the chute, and this appeared to be identical with the layer generated by the other feed method. It was therefore speculated that the loose, high-energy flows are often merely extended transients, even in cases where they survive for the restricted distance along this particular chute. With the porous plastic chute base used in the present work, these loose flows invariably collapsed into denser, slower moving layers within the length of the chute. In this case, therefore, it appears that only the dense flows correspond to fully developed conditions, so only results using the dense mode of feeding the chute, with control of flow by the slide valve at the exit of the pre-chute chamber, are reported.

For each chute inclination and flow rate the moving layer has an entry length, in which the depth increases or decreases, depending on the conditions, and an exit length in which the depth decreases on approaching the end of the chute. Measurements of depth, mass holdup, and velocity profile must, of course, be made in the section between these where the flow is ostensibly fully developed, provided such a section exists. This poses a limitation on the range of conditions that can be explored – for example, the exit length increases as the flow rate is decreased, and eventually eliminates the fully developed section. A longer chute would be desirable to ease this constraint. The range of flow rates that can be investigated is also constrained by the limited capacity of the pneumatic lift that returns the particles to the feed hopper. In the present work a number of runs are taken at flow rates in excess of this, so their duration is limited by depletion of the contents of the feed hopper. However, this is not serious, since steady flow conditions appear to be established quickly at the high flow rates in question.

## 5. Selection of parameter values

The theory contains a number of parameters characteristic of the particulate material and the solid boundaries with which it makes contact, together with the quantities  $\theta$ ,  $v^*$  and  $H/d$  which depend on the experimental conditions. In principle, the values of the material parameters can be determined by independent experiments, and this was attempted in the present case.

The angle of internal friction  $\phi$  was measured by shearing a sample of the material under a defined normal load in a standard 'Jenike' shear cell tester, and was found to be  $28.5^\circ$ . The angle of friction  $\delta$  between the material and the base of the chute was found by loading the chute at zero angle of inclination with a layer of the beads, then slowly increasing the inclination until the layer just began to slide steadily down the chute. The corresponding angle of inclination was taken as an estimate of  $\delta$ . In practice, it proved difficult to identify  $\delta$  accurately by this method, as there was a tendency for individual particles to roll (rather than slide) down the chute before the layer as a whole began to slide. However, sliding certainly began at an inclination between  $13^\circ$  and  $15^\circ$ , so a value of  $14^\circ$  was assigned to  $\delta$ .

The coefficients of restitution,  $e$  and  $e_w$ , were determined by dropping individual beads from a known height onto a sheet of glass or a piece of the porous polypropylene sheet. The required coefficients were then found by comparing the height of fall with a measured height of rebound. This measurement was not entirely satisfactory. For repeated drops from the same initial height there was quite a wide distribution of rebound heights, either because of rotation, or as a result of inhomogeneity in the sheet of material from which the particles bounce. Also, it is well established that coefficients of restitution are not constants, but depend quite strongly on the relative velocity at impact. It would, therefore, be most appropriate to measure them at impact velocities typical of collisions occurring in the flowing layer on the chute. But these are expected to be of the order of 10 cm/s, which is achieved only with a very small drop height, and correspondingly large percentage error in measuring the rebound height. For practical reasons, therefore, the rebound experiments were carried out with a much larger drop height (68 cm), giving estimates of 0.8 and 0.5 for  $e$  and  $e_w$ , respectively.

The specularity factor  $\phi'$  is determined by the nature of surface irregularities of the chute base on a scale comparable with the particle size. It is, therefore, distinct from  $\delta$ , which measures the tangential force exerted between the base and particles sliding on it, and  $e_w$ , which measures the loss in kinetic energy of a particle that collides with the base. In principle, an estimate of  $\phi'$  could be obtained by measuring the scattering of rebound directions for particles impacting the base at various angles of incidence, but the measurements would be tedious and difficult to perform at the low impact velocities which are typical for a base in contact with a flowing layer of particles. Thus our theoretical predictions were made for more than one value of this parameter to check the sensitivity of the results, and other calculations were carried out specifically to explore parameter sensitivity, as described below. Though  $\phi'$  can take any value between zero and unity, and this whole range is covered in our exploration of sensitivity (see figure 5), in practice values between 0.2 and 0.6, depending on the nature of the chute base, seem to give predictions that match experimental observations for the bases used in this and earlier work.

The dependence of the frictional normal stress  $N_f$  on bulk density has not been measured in detail for the type of material used here, though results of Scarlett & Todd (1969) suggest that it is negligible below some volume fraction  $\nu_1$  and increases

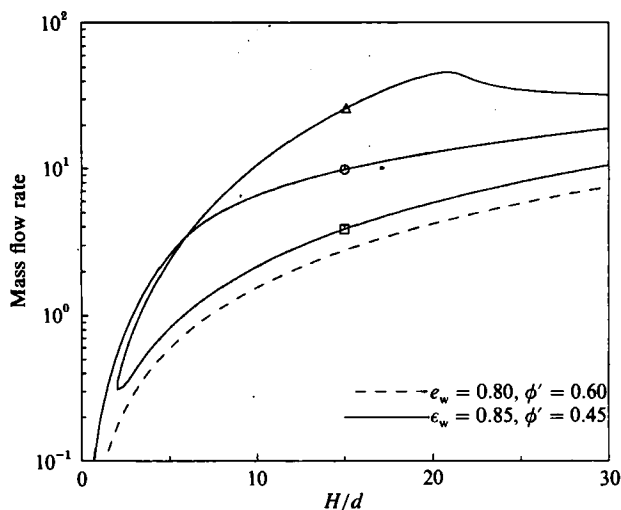


FIGURE 2. Mass flow rate versus  $H/d$  for the rough-based chute without aeration using 1 mm glass beads.  $\phi = 28.5^\circ$ ,  $\delta = 15^\circ$ ,  $e = 0.91$ ,  $\theta = 18^\circ$ .  $Fr$ ,  $P$  and  $N$  as in table 1.

$d$	0.1 cm
$\rho_p$	2.9 g/cm <sup>3</sup>
$\phi$	28.5°
$\delta$	14° ± 1°
$e$	0.8 ± 0.1
$e_w$	0.4–0.55 (0.5 chosen)
$Fr$	0.5 g/cm s <sup>2</sup>
$P$	2
$N$	5
$\phi'$	not measured

TABLE 1. Experimental parameter values

very rapidly as  $\nu$  approaches  $\nu_0$ . The simple algebraic form shown in (11) above has been adopted in the present work, with  $\nu_1 = 0.5$ ,  $Fr = 0.5$  g/cm s<sup>2</sup>,  $P = 2$  and  $N = 5$ . This is the same as the form used by Johnson *et al.* (1990) in treating the unaerated chute.

The above parameter values, together with the size and intrinsic density of the glass beads, are summarized in table 1.

The sensitivity of the solution to the choice of parameter values is well illustrated by the results of some computations for a chute without aeration, and with rather a rough base plate, corresponding to  $\delta = 15^\circ$ . Other parameters were  $\phi = 28.5^\circ$ ,  $e = 0.91$ , while the values of  $Fr$ ,  $P$  and  $N$  matched those in table 1. Figure 2 shows the calculated dimensionless mass flow rate, defined by

$$\dot{m} = \frac{1}{d(gd)^{\frac{1}{2}}} \int_0^H \nu u \, dy, \quad (29)$$

as a function of the dimensionless depth,  $H/d$ , for an angle of inclination of  $18^\circ$ . Results are shown for two pairs of values of the wall parameters  $e_w$  and  $\phi'$ , namely (0.8, 0.6) and (0.85, 0.45), and the difference is striking. For the former pair of values

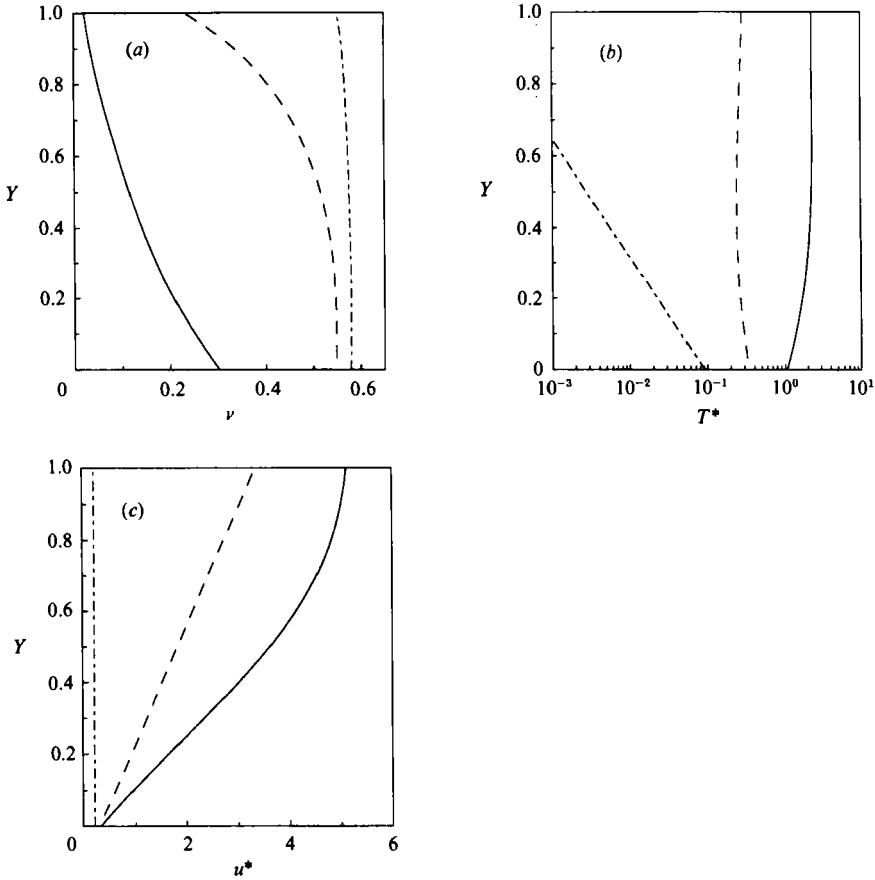


FIGURE 3. Profiles of (a) volume fraction, (b) particle temperature and (c) velocity for the rough-based chute without aeration at  $H/d = 15$ . Conditions correspond to the marked points in figure 2: —,  $\odot$ ; ---,  $\triangle$ ; - · - ·,  $\square$ .

$\dot{m}$  simply increases monotonically with  $H/d$ , as might be expected intuitively. For the latter pair, on the other hand, the flow rates are larger, and there are three widely spaced branches of solutions. The nature of these solutions can be seen in figure 3, which shows profiles of volume fraction, particle temperature, and velocity in the flowing layer for each of the three branches at a common value of the depth of the flowing layer, namely  $H/d = 15$ .

These quite modest changes in the values of the parameters  $\phi'$  and  $e_w$  have changed the form of the flow rate curves completely, so it is interesting to investigate further the effect of varying these parameters. Figures 4 and 5 show the effect on the mass flow rate of varying the parameters  $e_w$  and  $\phi'$ , respectively. In figure 4 the dependence of  $\dot{m}$  on  $e_w$  is plotted for  $\phi' = 0.60$  and for  $\phi' = 0.45$ . For  $\phi' = 0.60$  the results are not at all sensitive to the value of  $e_w$ , but for  $\phi' = 0.45$  there is a range of values of  $e_w$  over which the flow rate is very sensitive to this parameter, and multiple steady states exist. The multiplicity seen in figure 2 belongs to this range. In figure 5, where  $\dot{m}$  is plotted against  $\phi'$  for  $e_w = 0.85$ , a similar phenomenon is observed. There is a range of values of  $\phi'$  over which the flow rate is very sensitive to this parameter, and multiple steady states exist. The situation is, therefore, complicated and we do not know which branches represent stable states when there is

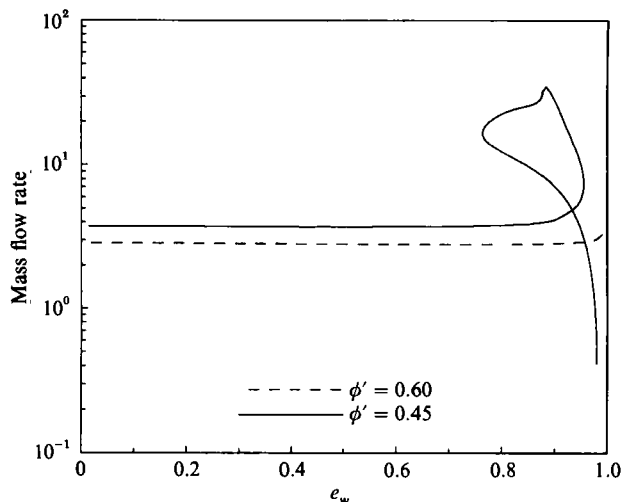


FIGURE 4. Dependence of mass flow rate on the choice of value for  $e_w$ . Other parameter values as for figure 2, and  $H/d = 15$ .

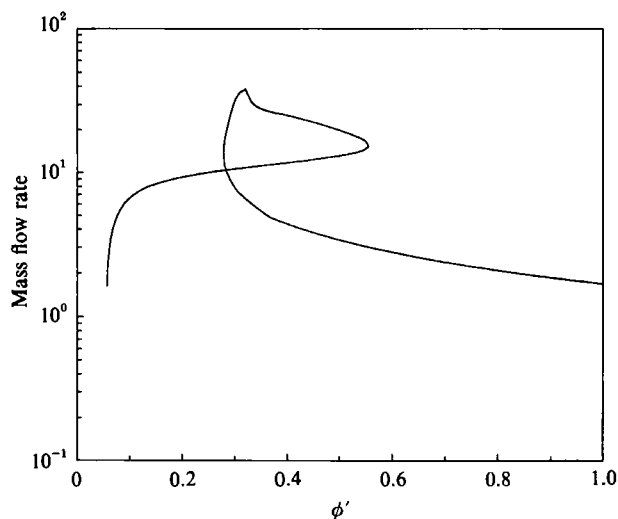


FIGURE 5. Dependence of mass flow rate on the choice of value for  $\phi'$ . Other parameter values as for figure 2, and  $H/d = 15$ ,  $e_w = 0.85$ .

multiplicity. The system may, or may not be sensitive to the value of a particular parameter, depending on the values taken by other parameters, and in view of figures 4 and 5 it would be unwise to make any general speculations about the form of curves showing the flow rate as a function of depth.

## 6. Experimental results and comparison with theory

The theory refers to a chute of infinite width normal to the direction of flow, while the separation of the lateral bounding walls of the experimental chute is only 6 cm, as noted above, so there is some doubt about whether the drag imposed on the

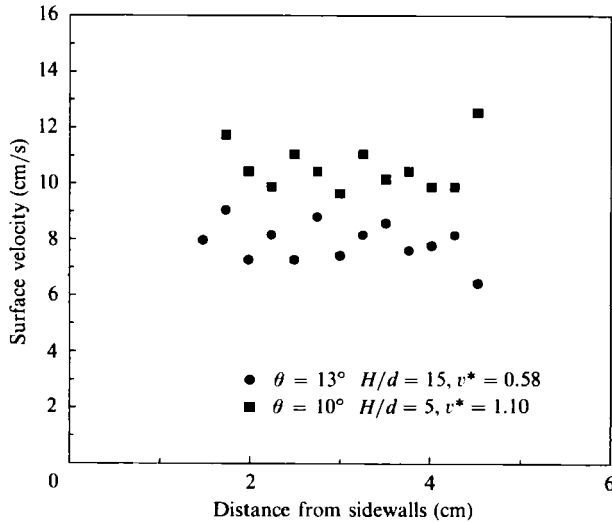


FIGURE 6. Measured transverse velocity profiles at the free surface of the flowing layer of 1 mm glass beads in the aerated chute at the conditions indicated.

flowing material by the walls can be neglected. Some idea of the influence of the walls can be obtained by determining the velocity profile for the particles in the free upper surface of the flowing layer, using the fibre-optic probe mounted above the layer, with its tip just clear of the moving surface. A number of profiles were determined in this way, and figure 6 shows two of these, both for flows with aeration. In each case the velocity profile shows little evidence of curvature over the rather limited part of the width accessible to the probe, whose casing prevents it from being located close to a wall. However, in the case of a granular material, the absence of marked curvature in the transverse velocity profile is not a guarantee that wall effects are small, since the material can be moving *en bloc*, in which state it is capable of transmitting shear stress from the wall without showing any curvature of the velocity profile.

Figures 7 and 8 show the main results of this work, namely experimental measurements and theoretical predictions of mass flow rate as a function of depth, at four values of the chute inclination and, for each value of the inclination, at various air flow rates. At the two higher values of the inclination, such that  $\theta > \delta$ , fully developed flow is possible even in the absence of aeration, but for the two lower values of the inclination, with  $\theta < \delta$ , there is no flow without aeration. In all the cases studied experimentally the mass flow rate increases monotonically with the depth of the flowing layer, and there is no indication of multiple states, in either the measurements or the theoretical predictions. (However, we have seen earlier that the theory certainly predicts multiplicity for other combinations of parameter values.) For a given depth the flow is also increased substantially by increasing the aeration rate, this enhancement becoming larger as  $H/d$  is increased. From a practical point of view the most important effect of aeration is to permit flow at smaller inclinations than could be used without aeration. Figure 7(c) shows that less than half the theoretical flow of air for minimum fluidization is needed to give steady flows at an inclination of  $13^\circ$ , but when this is reduced to  $10^\circ$  enough air for complete fluidization is needed to mobilize the material fully.

In figures 7(a-d) the curves showing the theoretical predictions were computed

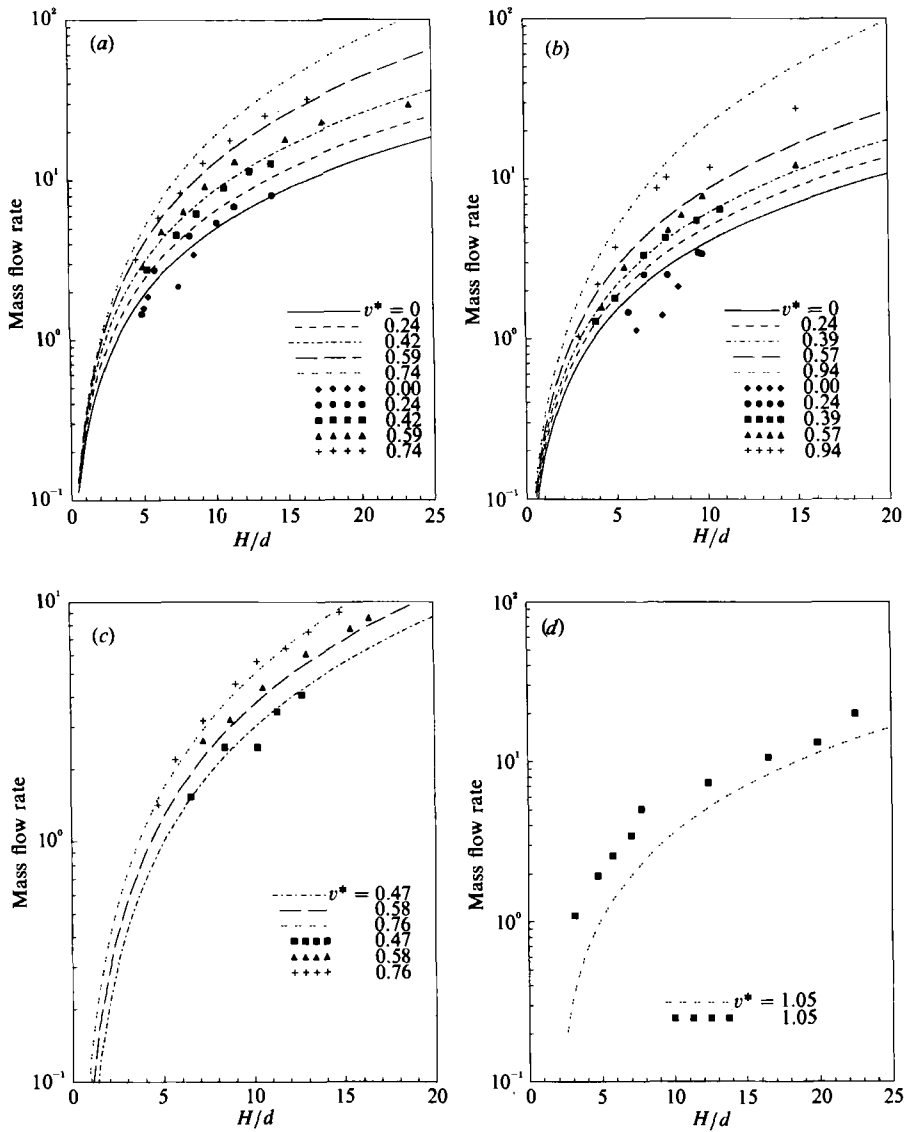


FIGURE 7. Mass flow rate versus  $H/d$  for the aerated chute at an inclination of (a)  $17^\circ$ , (b)  $16^\circ$ , (c)  $13^\circ$  and (d)  $10^\circ$ , and the indicated aeration rates. Theoretical curves for parameter values in table 1 with  $\phi' = 0.2$ .

using parameter values from table 1, with  $\phi' = 0.2$ , and the agreement between theory and observations is reasonably good except at  $\theta = 10^\circ$ , where the flow rates are underestimated by about a factor of two. The qualitative behaviour predicted corresponds to that observed, with the flow for each aeration rate increasing monotonically with depth, and the curves for different aeration rates fanning out as the depth increases. However, the quantitative success of the predictions should not be taken too seriously. As shown in figure 8, if the value assumed for  $\phi'$  is changed from 0.2 to 0.6, the measured flow rates are underestimated by a wide margin, though their qualitative features are still predicted correctly. Though the results are not presented here, corresponding computations with  $\phi' = 0.6$  for the other values of the chute inclination also show comparable underestimation of the flow rate.

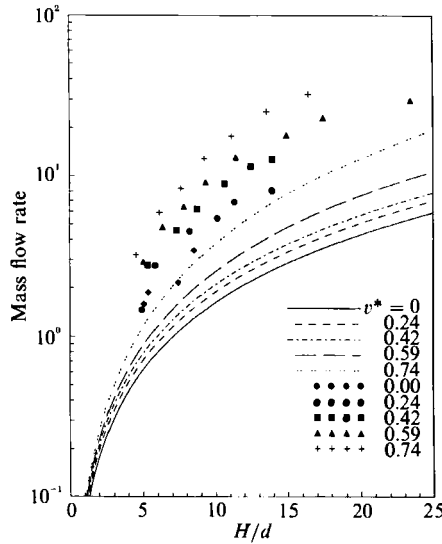


FIGURE 8. Mass flow rate versus  $H/d$  for the aerated chute at an inclination of  $17^\circ$  and the indicated aeration rates. Theoretical curves for parameter values in table 1 with  $\phi' = 0.6$ .

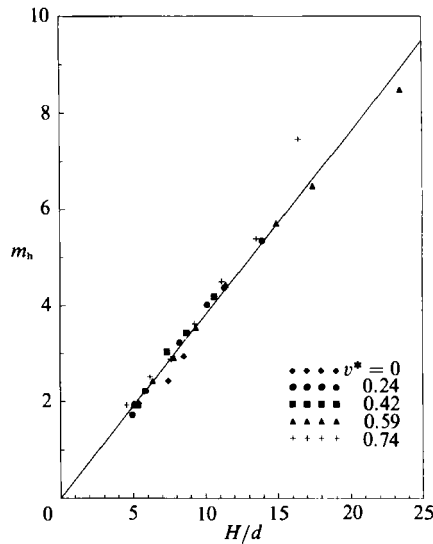


FIGURE 9. Mass holdup versus  $H/d$  for the aerated chute at an inclination of  $17^\circ$  and the indicated aeration rates. Also shown is the straight line through the origin which best fits all the data.

For each run the mass holdup  $M_h$  was measured by the method described above. The measurements are regarded as less reliable than those of the depth,  $H$ , because the sliding plates used to measure the holdup were placed quite close to the end of the chute, where exit effects were sometimes clearly significant. This was most serious at small chute inclinations, where the exit length was founded to be longest, so results are reported only for the largest inclination,  $\theta = 17^\circ$ . These are presented in figure 9 as a plot of the dimensionless holdup  $m_h = M_h/WLd\rho_p$  against  $H/d$ , where  $W$  is the width of the chute and  $L$  the distance between the sliding plates used to measure the holdup. The ratio of  $m_h$  to  $H/d$  is equal to  $\nu$ , the mean volume fraction

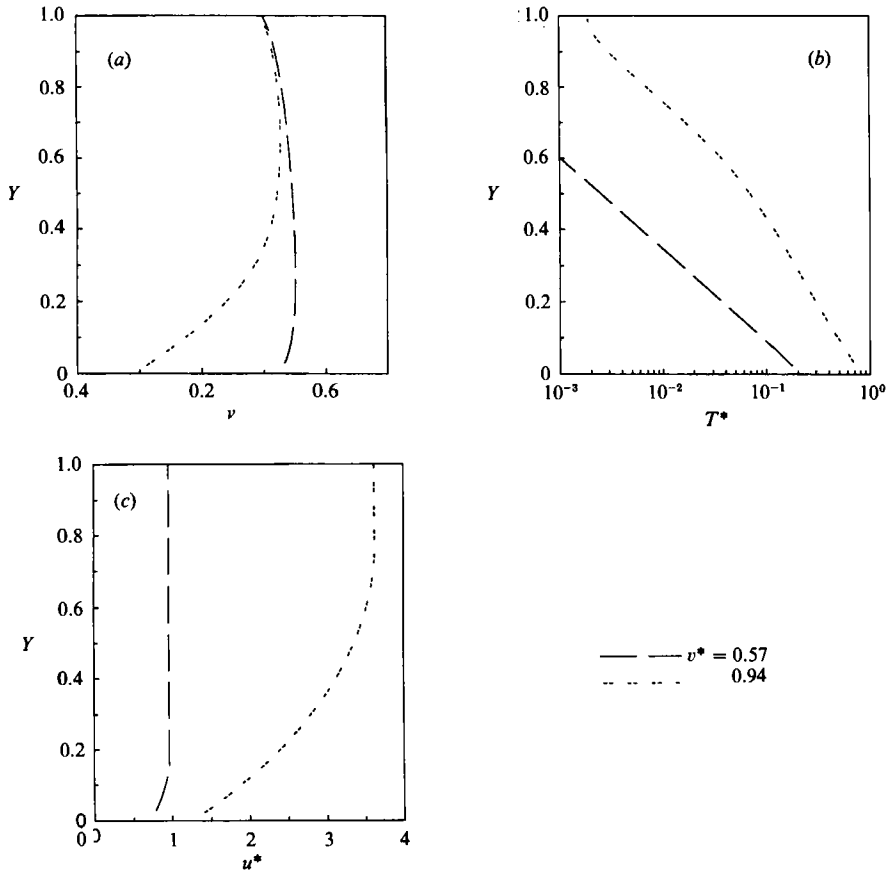


FIGURE 10. Profiles of (a) volume fraction, (b) particle temperature and (c) velocity for the aerated chute at an inclination of  $16^\circ$ , with  $H/d = 15$ , and at the indicated aeration rates. Parameter values as in table 1, with  $\phi' = 0.2$ .

of solids in the flowing layer, so the fact that the data are well represented by a single straight line through the origin shows that the mean volume fraction is essentially independent of the flow rate and the aeration rate for a chute of this inclination. The slope of the best line, shown in the diagram, is 0.38, and this gives the average value of  $\nu$ . It is clear from these results that the effect of aeration is not to expand the particulate material, but to relieve the buildup of stress within the layer due to the weight of the overburden. Correspondingly, the plots of mass flow rate versus depth show that the depth of the flowing layer *decreases* as the aeration rate is increased, at a given value of the mass flow rate.

Figures 10, 11 and 12 show some computed profiles of volume fraction, particle temperature and velocity at inclinations of  $16^\circ$ ,  $13^\circ$  and  $10^\circ$ , respectively, for aerated flows. From figure 10, at the lower aeration rate the material is seen to move as a block, with volume fraction approximately 0.58, superimposed on a relatively thin layer of shearing material in contact with the base of the chute. The particle temperature decreases monotonically on moving up from the base, showing that pseudothermal energy is being generated as the material slips over the base, then conducted upward through the flowing layer. At the higher aeration rate particle temperatures are a good deal higher, the shearing zone adjacent to the base now

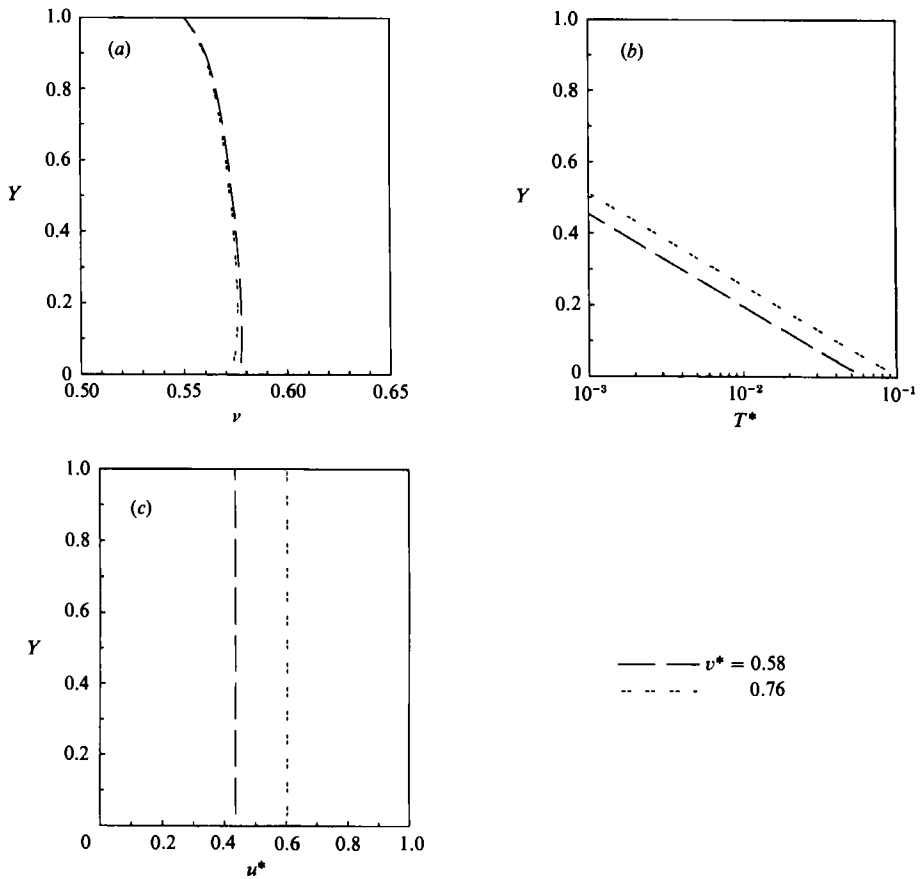


FIGURE 11. Profiles of (a) volume fraction, (b) particle temperature and (c) velocity for the aerated chute at an inclination of  $13^\circ$ , with  $H/d = 15$ , and at the indicated aeration rates. Parameter values as in table 1, with  $\phi' = 0.2$ .

extends upward through about half the total depth, and the volume fraction of solids is reduced substantially in this shearing zone. Figure 11 shows a similar pattern of behaviour, but at this lower inclination velocities are smaller, particle temperatures are lower, and the shearing zone of reduced bulk density is now confined to a thinner layer adjacent to the base. The reduction in bulk density within that zone is also quite small. At  $10^\circ$  inclination figure 12 shows that essentially the whole flowing layer is in plug flow. The shearing layer adjacent to the base still exists, but is too thin to show up in the plotted velocity profiles, though a hint of its presence can be seen in the small reduction of bulk density very close to the base. As might be expected, particle temperatures are now quite low, with thermal activity confined to the lower part of the layer. These results are all in accord with what would be expected from earlier work on unaerated chutes (Johnson *et al.* 1990), together with the anticipated effects of aeration.

## 7. Concluding remarks

The theoretical treatment is based on equations of motion which are incomplete in a number of ways, and certain aspects of the particular boundary-value problem studied have also been neglected. As emphasized from the beginning, the rheological

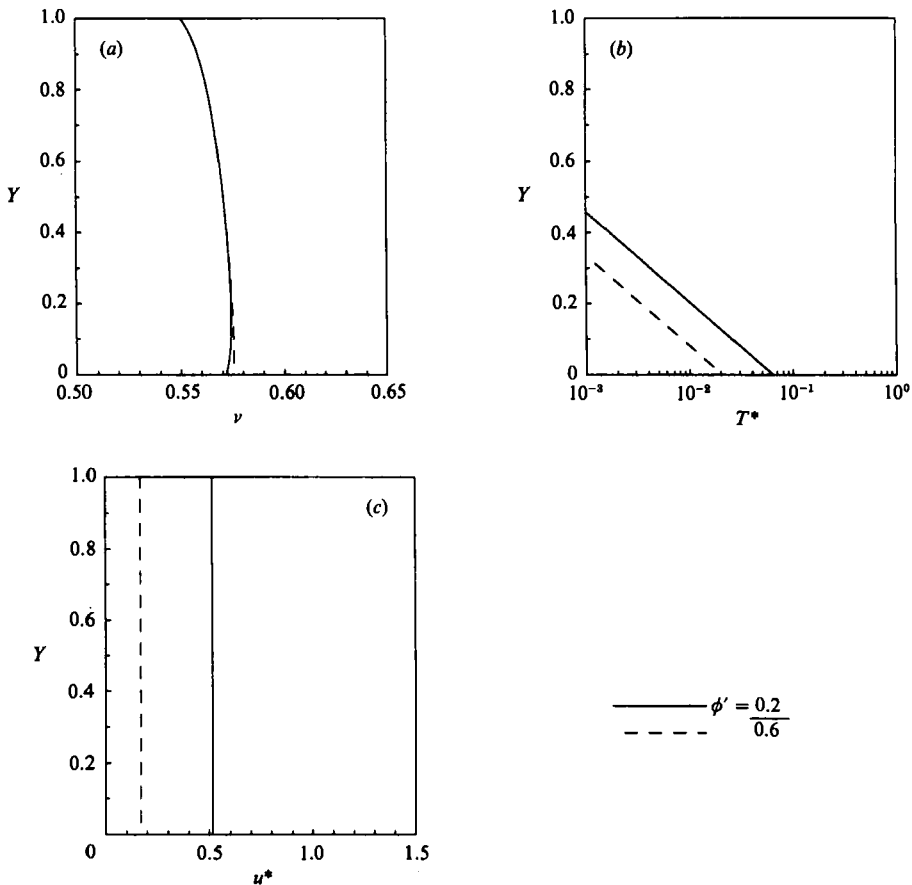


FIGURE 12. Profiles of (a) volume fraction, (b) particle temperature and (c) velocity for the aerated chute at an inclination of  $10^\circ$ , with  $H/d = 15$ , and at an aeration rate  $\nu^* = 1.05$ . Curves correspond to the two indicated values of  $\phi'$ .

model used for stress in the flowing particulate material is no more than a naive additive combination of two quite disparate limiting cases, one drawn from soil mechanics for the behaviour at high bulk density and slow shear rate, the other based in kinetic theory for the behaviour at lower density and higher shear rate. In addition, the only aspect of the interaction of the particles with the interstitial air that has been taken into account is a drag force depending on their relative convective velocities. It is also clear that the presence of the interstitial air influences the nature of collisions between particles, and it is known that the pseudo-thermal random component of the particle motion may either draw energy from the resulting motion relative to the air, or be damped by losing energy. All these effects have been neglected. Furthermore, and particular to the geometry of the problem considered, the presence of lateral bounding walls has been neglected, as has the drag exerted on the particles as they accelerate the air entering through the porous plate.

On the experimental side, though all the parameters appearing in the equations of motion can, in principle, be measured by independent experiments, we have seen that this is not always easy. In particular, we lack any independent value for the specularity coefficient  $\phi'$  appearing in the momentum boundary condition at the wall, and there is really no parameter whose value has been found with adequate precision.

This is unfortunate since, as we have shown, the results can be very sensitive to certain parameter values over limited ranges of operating conditions. Nevertheless, accepting the best independent measurements we have for all the parameters other than  $\phi'$ , it has been shown that the correct qualitative behaviour is predicted for two widely different values of  $\phi'$ , one of which also gives quite good quantitative predictions.

The results clearly indicate that the properties of the solid boundary play a very important role in determining the nature of the flow. The boundary may act as a source or sink of pseudo-thermal energy, and the sign and magnitude of this energy flux is sensitive to the values of the parameters  $e_w$  and  $\phi'$ . Changing the aeration rate within the limits we have studied does not dilate the flowing material very much, but it does increase the slip velocity at the boundary, and consequently the particle temperature throughout the flowing layer. The magnitudes of both shear and normal stresses are then reduced, and a higher proportion of these stresses is generated by the collisional, rather than the frictional mechanism. Thus, the investigation of shear flow has been extended by aeration to cases where the bulk density is high but the transmitted stresses are low; a situation not easy to realize in other ways.

This work has been supported by the United States Department of Energy under Grant No. DE-FG22-86PC90518. It also forms part of a larger programme on various aspects of the motion of particulate systems, which has received continuing support from the National Science Foundation, Fluid, Particulate and Hydraulic Systems Program, under Grant No. 8504201. During the later stages of the work the second author was a Visiting Professor at Rice University, which provided a welcome opportunity for uninterrupted study.

#### REFERENCES

- DOEDEL, E. 1986 *Software for Continuation and Bifurcation Problems in Ordinary Differential Equations*. (AUTO Software Package user's manual.)
- JENKINS, J. T. 1987 Rapid shear flows of granular materials. In *Non-classical Continuum Mechanics: Abstract Techniques and Applications* (ed. R. J. Knops & A. A. Lacey). Cambridge University Press.
- JOHNSON, P. C. & JACKSON, R. 1987 Fractional-collisional constitutive relations for granular materials, with application to plane shearing. *J. Fluid Mech.* **176**, 67–93.
- JOHNSON, P. C., NOTT, P. & JACKSON, R. 1990 Frictional–collisional equations of motion for particulate flows and their application to chutes. *J. Fluid Mech.* **210**, 501–535.
- LUN, C. K. K., SAVAGE, S. B., JEFFREY, D. J. & CHEPURNIY, N. 1984 Kinetic theories for granular flow: inelastic particles in Couette flow and slightly inelastic particles in a general flow field. *J. Fluid Mech.* **140**, 223–256.
- NOTT, P. 1991 Analysis of granular flow in aerated and vibrated chutes. Ph.D. dissertation, Princeton University.
- RICHARDSON, J. F. 1971 Incipient fluidization and particulate systems. In *Fluidization* (ed. J. F. Davidson & D. Harrison). Academic.
- SAVAGE, S. B. 1982 Granular flow down rough inclines – review and extension. In *Proc. US-Japan Seminar on New Models and Constitutive Relations in the Mechanics of Granular Materials* (ed. J. T. Jenkins & M. Satake). Elsevier.
- SCARLETT, B. & TODD, A. C. 1969 The critical porosity of free flowing solids. *Trans. ASME B: J. Engng Ind.* **91**, 477–488.